

# Photoproduction of $D^*$ Mesons and Jets with H1

Gero Flucke (on behalf of the H1 collaboration)

*DESY, Hamburg, Germany*

**Abstract.** Cross sections are measured for photoproduction events containing a  $D^{*\pm}$  meson and a jet. They are determined for photon-proton centre-of-mass energies  $171 < W < 256$  GeV and photon virtualities  $Q^2 < 0.01$  GeV<sup>2</sup>. A jet that does not contain the  $D^*$  meson is required. Differential cross sections are compared with perturbative QCD predictions in collinear and  $k_t$ -factorisation.

**Keywords:** Charm, Jets, Photoproduction, QCD, Cross sections

**PACS:** 12.38.Qk,13.60.Le,13.85.Hd,14.40.Lb

## INTRODUCTION

Inclusive  $D^*$  photoproduction at HERA is interesting as a general test of the charm production mechanism in high energy  $ep$  collisions. The measurements [1, 2, 3, 4] are consistent with the assumption that heavy quarks are predominantly produced via a photon-gluon fusion mechanism. The measurement of a  $D^*$ +jet pair gives the possibility to investigate further details of the charm production mechanism.

## DATA SELECTION

Data of the years 1999 and 2000 with an integrated luminosity of  $\mathcal{L} = 51.1$  pb<sup>-1</sup> are analysed where protons of  $E_p = 920$  GeV have been collided with positrons of  $E_e = 27.6$  GeV.  $D^{*\pm}$  mesons are reconstructed from tracks in the decay channel<sup>1</sup>  $D^{*+} \rightarrow D^0 \pi_s^+ \rightarrow K^- \pi^+ \pi_s^+$  as in [3]. Photoproduction is selected through the reconstruction of the scattered positron under a small angle  $(\pi - \theta) < 5$  mrad<sup>2</sup>, leading to photon virtualities of  $Q^2 < 0.01$  GeV<sup>2</sup> and photon-proton centre-of-mass energies of  $171 < W < 256$  GeV.

Jets are defined by the inclusive  $k_t$ -algorithm [5]. The input of the jet algorithm are hadronic-final-state objects (HFS) from combining tracks and calorimeter clusters. The HFS objects of the  $D^*$  decay tracks are replaced by the  $D^*$  candidate itself. The minimal required transverse momentum is  $p_t(\text{jet}) > 3$  GeV. A satisfying jet reconstruction even at these low values of  $p_t$  is achieved for jets in the central detector region  $|\eta(\text{jet})| < 1.5$  where well measured tracks dominate the HFS objects. The aim is to tag a second object besides the  $D^*$  from the hard process. Therefore the jet with the highest transverse momentum *not* containing the  $D^*$  meson is selected. In total a signal of  $588 \pm 46$   $D^*$ +jet combinations is observed. Details of the  $D^*$  and jet selection are described in [6].

---

<sup>1</sup> Charge conjugate states are always implicitly included.

<sup>2</sup> The polar angle  $\theta$  is measured with respect to the direction of the colliding protons.

**TABLE 1.** Parameters of the QCD calculations: renormalisation ( $\mu_r$ ) and factorisation ( $\mu_f$ ) scales, parton density parametrisations and charm fragmentation treatment.

	PYTHIA 6.1	CASCADE 1.2	FMNR	ZMVFNS
$\mu_r^2$	$m_c^2 + p_{t,c}^2$	$4m_c^2 + p_{t,c}^2$	$m_c^2 + (p_{t,c}^2 + p_{t,\bar{c}}^2)/2$	$m_c^2 + p_{t,D^*}^2$
$\mu_f^2$	$m_c^2 + p_{t,c}^2$	$Q_t^2 + \hat{s}$	$4(m_c^2 + (p_{t,c}^2 + p_{t,\bar{c}}^2)/2)$	$4(m_c^2 + p_{t,D^*}^2)$
$p$ -PDF	CTEQ5L [12]	A0 [13]	CTEQ5M [12]	
$\gamma$ -PDF	GRV-G LO [14]	–	GRV-G HO [14]	
Fragm.	Lund with $\varepsilon_{pet} = 0.078$		$\varepsilon_{pet} = 0.035$ [15]	BKK O [16]

## QCD CALCULATIONS

The results will be compared with two leading order calculations supplemented with parton showers, the collinear factorising PYTHIA 6.15 [7] and the  $k_t$ -factorising CASCADE 1.2 [8], as well as with collinear next-to-leading order (NLO) calculations in the massive (FMNR [9]) and massless (ZMVFNS [10]) scheme. The charm pole mass is set to  $m_c = 1.5$  GeV and the fragmentation fraction  $f(c \rightarrow D^*) = 0.235$  [11] is applied. The main parameters of all calculations are listed in table 1. For both NLO calculations corrections are applied to account for the transition from parton level to hadron level jets. They are obtained as bin-by-bin corrections calculated between parton and hadron level jets in PYTHIA. Uncertainties of the CASCADE, FMNR and ZMVFNS calculations are estimated by varying the charm mass and the factorisation and renormalisation scales.

## CROSS SECTIONS

To determine bin averaged differential cross sections, the numbers of reconstructed  $D^*$ +jet combinations, determined by fits to the  $\Delta m = m(K\pi\pi_s) - m(K\pi)$  distributions, is corrected for the branching ratio  $BR(D^* \rightarrow K\pi\pi_s) = 0.0257$  [17], limited acceptances, reconstruction and trigger inefficiencies. Systematic uncertainties amount to 15 – 17%. Their main contributions are the uncertainties in the track reconstruction efficiency.

The  $D^*$ +jet cross section are shown in figure 1 and compared with the predictions. The  $p_t(D^*)$  (fig. 1a+c) and  $p_t(\text{jet})$  (fig. 1e+h) distributions are rapidly falling towards higher transverse momenta and are reasonably well described by all QCD calculations, but the CASCADE prediction shows a slightly harder spectrum than observed in the data.

The cross sections as a function of the pseudorapidity of the jet and the  $D^*$  differ: The  $\eta(D^*)$  (fig. 1b+d) distribution falls off with increasing values of  $\eta$  whereas  $\eta(\text{jet})$  (fig. 1f+i) is almost flat. The difference is not caused by the different kinematic cuts for the  $D^*$  and the jet, but suggests that the jet cross section contains contributions from non-charm jets. They could arise from hard gluon radiation from the initial state, which mainly populates the forward (large  $\eta$ ) region. This hypothesis is also supported from comparison with the PYTHIA calculations: for direct photon processes ( $\gamma g \rightarrow c \bar{c}$ ) the  $\eta$  spectra of the jet and the  $D^*$  are found to be similar (figures 1b+f). Only after inclusion of the charm excitation processes, which effectively simulate processes like  $\gamma g \rightarrow c \bar{c} g$ , the  $\eta$  spectrum of the jet can be described. A similar feature is obtained with  $k_t$  factorisation as implemented in CASCADE, but also with the NLO calculations.

In the figures 1g+j the cross section is presented as a function of  $\Delta\phi(D^*,\text{jet})$ . For processes like  $\gamma g \rightarrow c\bar{c}$  a back-to-back configuration is expected. The large fraction of events where the  $D^*$  and the jet are not back-to-back suggests a significant contribution of higher order QCD radiation.

## CONCLUSIONS

Photoproduction of  $D^*$  mesons has been analysed at relatively low transverse momenta. Cross sections have been determined for events with a  $D^*$  meson and a jet not containing the  $D^*$ . The results have been compared with four approaches of QCD calculations.

The measured transverse momentum distributions of the  $D^*$  and jet are in general in agreement with the prediction within the theoretical uncertainties.

Comparing the pseudorapidity distributions of the  $D^*$  and the jet it is striking that the  $\eta(D^*)$  distribution falls in forward direction whereas  $\eta(\text{jet})$  is almost constant. This observation suggests that the jet cross section contains not only a charm jet but also a significant contribution from a further parton, most likely a gluon jet.

The azimuthal difference  $\Delta\phi(D^*,\text{jet})$  is sensitive to the amount of gluon radiation. The measured cross section shows that higher orders beyond the LO process  $\gamma g \rightarrow c\bar{c}$  with a collinear gluon contribute significantly. The  $\Delta\phi(D^*,\text{jet})$  is reasonably well described by calculations applying leading log parton showers in the collinear factorisation ansatz, or by using un-integrated gluon densities in the  $k_t$ -factorisation ansatz, but not by fixed order NLO calculations.

## ACKNOWLEDGMENTS

We would like to thank S. Frixione for the FMNR code and G. Heinrich for the ZMVFNS calculations.

## REFERENCES

1. C. Adloff, et al., *Nucl. Phys.*, **B545**, 21–44 (1999), hep-ex/9812023.
2. J. Abbiendi, et al., *Eur. Phys. J.*, **C6**, 67–83 (1999), hep-ex/9807008.
3. H1, Photoproduction of  $D^*$  Mesons at HERA, EPS03, H1prelim-03-071.
4. ZEUS, Measurement of  $D^*$  Photoproduction at HERA, ICHEP02, ZEUS-pre1-02-004.
5. S. Ellis, and D. Soper, *Phys. Rev.*, **D48**, 3160–3166 (1993), hep-ph/9305266.
6. G. Flucke, Ph.D. thesis, Universität Hamburg (2005), DESY-THESIS-2005-006.
7. T. Sjöstrand, et al., *Comput. Phys. Commun.*, **135**, 238–259 (2001), hep-ph/0010017.
8. H. Jung, *Comput. Phys. Commun.*, **143**, 100–111 (2002), hep-ph/0109102.
9. S. Frixione, P. Nason, and G. Ridolfi, *Nucl. Phys.*, **B454**, 3–24 (1995), hep-ph/9506226.
10. G. Heinrich, and B. A. Kniehl, *Phys. Rev.*, **D70**, 094035 (2004), hep-ph/0409303.
11. L. Gladilin, Charm hadron production fractions (1999), hep-ex/9912064.
12. H. L. Lai, et al., *Eur. Phys. J.*, **C12**, 375–392 (2000), hep-ph/9903282.
13. H. Jung, “Un-integrated Parton Density Functions in CCFM,” (DIS 2004), hep-ph/0411287.
14. M. Glück, E. Reya, and A. Vogt, *Phys. Rev.*, **D46**, 1973–1979 (1992).
15. P. Nason, and C. Oleari, *Nucl. Phys.*, **B565**, 245–266 (2000), hep-ph/9903541.
16. J. Binnewies, B. A. Kniehl, and G. Kramer, *Phys. Rev.*, **D58**, 014014 (1998), hep-ph/9712482.
17. S. Eidelman, et al., *Phys. Lett.*, **B592**, 1 (2004).

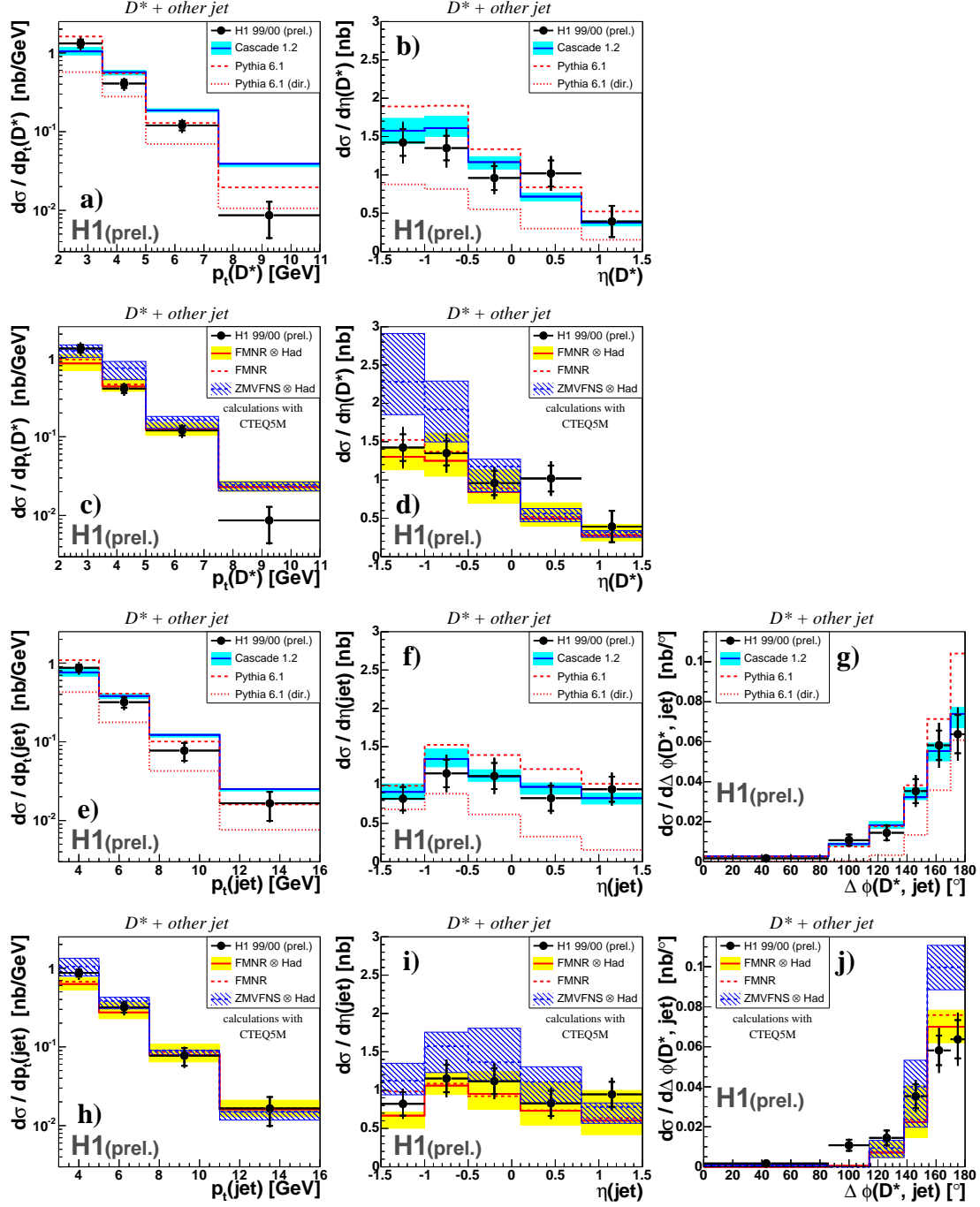


**FIGURE 1.**  $D^*$ +jet cross sections in bins of the transverse momentum (left column) and pseudorapidity (middle column) of the jet and the  $D^*$  and their azimuthal distance  $\Delta\phi(D^*, \text{jet})$  (right column) compared with the predictions of PYTHIA and CASCADE (a-b,e-g) and of the next-to-leading order calculations FMNR and ZMVFS (c-d,h-j). For PYTHIA the direct contribution of the prediction is shown separately and labelled as “dir.”. The central FMNR prediction is shown before and after applying the hadronisation corrections. The inner error bars of the data indicate the statistical uncertainties, the outer error bars indicate the statistical and systematic uncertainties added in quadrature.